Neurobiology of Disease 176 (2023) 105930

Contents lists available at ScienceDirect

Neurobiology of Disease

journal homepage: www.elsevier.com/locate/ynbdi

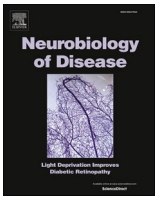

Selective activation of striatal indirect pathway suppresses levodopa induced-dyskinesias

Iván Castela [a,b,c], Raquel Casado-Polanco [a], Yaiza Van-Waes Rubio [a], Joaquim Alves da Silva [g], Raquel Marquez [a,b], Beatriz Pro [a,b], Rosario Moratalla [e], Peter Redgrave [f], Rui M. Costa [g,h], José Obeso [a,b,d], Ledia F. Hernandez [a,b,d,*]

[a] HM-CINAC, (Centro Integral de Neurociencias Abarca Campal), Hospital Universitario HM Puerta del Sur, HM Hospitales, Madrid, Spain
[b] Network Center for Biomedical Research in Neurodegenerative Diseases (CIBERNED), Carlos III Health Institute, Madrid, Spain
[c] PhD Program in Neuroscience, Autonoma de Madrid University, Madrid 28029, Spain
[d] Universidad CEU-San Pablo, Madrid, Spain
[e] Instituto Cajal-CSIC, Madrid, Spain
[f] Department of Psychology, University of Sheffield, Sheffield S10 2TN, UK
[g] Champalimaud Research, Champalimaud Centre for the Unknown, Lisbon 1400-038, Spain
[h] Departments of Neuroscience and Neurology, Zuckerman Mind Brain Behavior Institute, Columbia University, New York, NY 10027, USA

ARTICLE INFO

Keywords:
Parkinson's disease
Dyskinesia
LIDs
Striatum
Optogenetics

ABSTRACT

Levodopa (L-DOPA) administration remains the gold standard therapy for Parkinson's disease (PD). Despite several pharmacological advances in the use of L-DOPA, a high proportion of chronically treated patients continues to suffer disabling involuntary movements, namely, L-DOPA-induced dyskinesias (LIDs). As part of the effort to stop these unwanted side effects, the present study used a rodent model to identify and manipulate the striatal outflow circuitry responsible for LIDs. To do so, optogenetic technology was used to activate separately the striatal direct (D1R- expressing) and indirect (D2R- expressing) pathways in a mouse model of PD. Firstly, D1-cre or A2a-cre animals received unilateral injections of neurotoxin 6-hydroxydopamine (6-OHDA) to simulate the loss of dopamine observed in PD patients. The effects of independently stimulating each pathway were tested to see if experimental dyskinesias could be induced. Secondly, dopamine depleted A2a-cre animals received systemic L-DOPA to evoke dyskinetic movements. The ability of indirect pathway optogenetic stimulation to suppress pre-established LIDs was then tested. Selective manipulation of direct pathway evoked optodyskinesias both in dopamine depleted and intact animals, but optical inhibition of these neurons failed to suppress LIDs. On the other hand, selective activation of indirect striatal projection neurons produced an immediate and reliable suppression of LIDs. Thus, a functional dissociation has been found here whereby activation of D1R- and D2R-expressing projection neurons evokes and inhibits LIDs respectively, supporting the notion of tight interaction between the two striatal efferent systems in both normal and pathological conditions. This points to the importance of maintaining an equilibrium in the activity of both striatal pathways to produce normal movement. Finally, the ability of selective indirect pathway optogenetic activation to block the expression of LIDs in an animal model of PD sheds light on intrinsic mechanisms responsible for striatal-based dyskinesias and identifies a potential therapeutic target for suppressing LIDs in PD patients.

1. Introduction

Parkinson's disease (PD) is principally characterized by the loss of dopamine-containing neurons in the Substantia nigra *pars compacta* (SNpc) and the subsequent loss of dopamine in the striatum. Depletion of striatal dopamine is a principal cause of the cardinal signs (i.e. bradykinesia, resting tremor, rigidity) of PD (Kalia and Lang, 2015). Currently, levodopa (L-DOPA) remains the most widely prescribed treatment to alleviate these manifestations. However, L-DOPA-induced dyskinesias (LIDs) remain a frequent side-effect associated with chronic levodopa treatment. In some patients these involuntary movements may be so incapacitating that additional interventions, including surgery, are

* Corresponding author at: HM-CINAC, Hospital Universitario HM Puerta del Sur, Avda. Carlos V, 70, 28938-Mostoles, Madrid, Spain.
E-mail address: lediafhernandez@hmhospitales.com (L.F. Hernandez).

https://doi.org/10.1016/j.nbd.2022.105930
Received 2 August 2022; Received in revised form 16 November 2022; Accepted 18 November 2022
Available online 19 November 2022

required to achieve effective therapeutic control (Espay et al., 2018).

Medium spiny neurons (MSNs) represent 95% of the total striatal neuronal population. MSNs can be divided in two subtypes depending on the expression of sub-classes of dopamine receptors. Thus, D1R-expressing MSNs project directly to basal ganglia output nuclei (internal globus pallidus and substantia nigra *pars reticulata*) and are known as the "direct pathway" (D1-MSNs), whereas D2R-expressing MSNs project indirectly to basal ganglia output nuclei (via the external globus pallidus) and are known as the "indirect pathway" (D2-MSNs) (Albin et al., 1989). Dopaminergic activation of direct pathway MSNs and inhibition of indirect pathway MSNs are required for an adequate motor output.

While D1-MSNs have been hypothesized to play an important role in LIDs (Pavón et al., 2006; Cenci, 2007), the possible engagement of D2-MSNs in striatal dyskinesias remains unknown. Unbalanced activity between striatal pathways during dyskinesia has been described, with hyperactivity of D1-MSNs and hypoactivity of D2-MSNs (Parker et al., 2018; Ryan et al., 2018; Suárez et al., 2018). Additionally, photo- and chemostimulation of D1-MSNs elicits abnormal movements that resemble LIDs (Alcacer et al., 2017; Ryan et al., 2018; Keifman et al., 2019) while deletion of D1R abolishes them (Darmopil et al., 2009). These findings support a causal role for D1-MSNs in the expression of LIDs and suggest an imbalance between the pathways could be the crucial element.

These results also fit well with the classical model of basal ganglia function, where activity of the direct pathway facilitates movement while activity of the indirect pathway inhibits movement (Kravitz et al., 2010; Freeze et al., 2013). However, recent studies have challenged this traditional view. Specifically, new experimental data indicate both pathways are engaged during the initiation of movements (Cui et al., 2013; Klaus et al., 2017; Parker et al., 2018) and we have reported previously, that co-activation of both direct and indirect pathways produced dyskinesia in dopamine depleted rats (Hernandez et al., 2017). Moreover, activation of the indirect pathway during movement was also shown in FosTRAP mice, where 10% of the neurons activated by L-DOPA during classical LIDs were D2R- expressing neurons (Girasole et al., 2018).

The aim of the present study was, therefore, first to gain further insight into the role played by each of the direct and indirect striatal pathways in the generation of dyskinesias. Secondly, we sought to test whether treating the imbalance in activity between the pathways could suppress dyskinetic movements. We found that selective direct pathway activation elicited dyskinetic movements, whereas experimental LIDs were blocked by selective activation of the indirect pathway.

2. Methods

2.1. Animals

All experimental procedures were approved by the HM-CINAC Committee on Animal Care and Champalimaud Centre for the Unknown Ethical Committee in accordance with the National Research Council's Guide for the Care and Use of Laboratory Animals (RD 53/2013) and European Community guidelines (2003/65/CE). This study was performed in heterozygous adult BAC Drd1a-Cre and Adora2a-Cre transgenic male mice (n = 39, 12–20 weeks old.). Animals were housed individually, with food and water ad libitum, on a normal diurnal light cycle (lights on: 9:00 A.M.–9:00 P.M.). All experiments were performed during the light period. The genotyping experimental development was provided by the Genomics and NGS Core Facility at the Centro de Biología Molecular Severo Ochoa (CBMSO, CSIC-UAM) which is part of the CEI (UAM + CSIC), Madrid, Spain.

2.2. Surgical procedures

Animals were deeply anesthetized with a mixture of ketamine (100 mg/kg) and xylazine (10 mg/kg, i.p.). 6-hydroxydopamine (6-OHDA hydrobromide; 5 μg (1 μl, 5 mg/ml), Sigma Aldrich) or saline was injected unilaterally (0.2-μl/min) into the right medial forebrain bundle (MFB) (AP: −1 mm, ML: −1 mm from bregma; and DV: −4.9 mm from dura). The viral vectors carrying the channelrhodopsin AAV2-EF1a-DIO-hChR2(H134R)-EYFP-WPRE (4.2×10^{12} viral particles/ml, Vector Core, North Carolina University, USA). or halorhodopsin AAV2-EF1a-DIO-eNpHR3.0-EYFP (1×10^{12} viral particles/ml, Vector Core, North Carolina University, USA) were injected (1 μl) into the right dorsolateral striatum (Bregma, AP: +0.5 mm; ML: −2.5 mm; DV: −2.5 mm (from dura)) at a flow rate 0.1 μl/min. Hamilton syringes were left in place for 5 and 10 min after 6-OHDA/saline and viral injections, respectively. An optic fiber (length: 3.5 mm; diameter: 200 μm, NA: 0.22; Thorlabs, NJ, USA) was placed 300 μm above the virus injection site. This was anchored to the animal's skull with a small screw (JI Morris, MA, USA) and dental cement (Lang Dental Manufacturing Co., Inc., France). Dopamine depleted animals received special post-operative care. To prevent dehydration, mice received glucose-saline solution (0.1 ml/10 g, s.c) along with hydration gel once a day for 2–3 weeks (Francardo et al., 2011).

2.3. Optogenetic experiments

Four weeks after surgery, animals were habituated to a glass cylinder (17 cm diameter) and the patch cables were connected for 10–15 min for 2 days. TTL- controlled blue light (CNI, 300 mW, 473 nm, China) and yellow light (CNI, 100 mW, 589 nm, China) lasers were calibrated before every experiment and delivered using a pulse generator (CS-420, CIBERTEC, Madrid, Spain). Light intensity was calibrated daily using an optic fiber, like the one implanted, and a power meter (ThorLabs, PM100D and S121C). The illuminating power was adjusted at the patch cord to 51.19 mW/mm^2 for ChR2 and 78.76 mW/mm^2 for eNpHr3.0 experiments.

Different sets of experimental protocols were used: Ten second continuous light application was chosen based on previous optogenetic experiments (Hernandez et al., MDJ,2017), and recording experiments showing that neurons stop responding after 5-10s of light stimulation (data not published). The stimulation frequency of 10 Hz was chosen after Perez et al., 2017. The timing of the stimulation protocols was as follows (Fig. 1A):

A – (referred to as continuous protocol), a three-minute baseline period followed by nine intervals of ten seconds with continuous blue laser stimulation separated by 30 s inter-stimulation intervals. This protocol was aimed to stimulate a broader neuronal population.

B – (referred to as 10 Hz protocol) a baseline period of three minutes followed by three minutes with 10 Hz stimulation (20 ms pulse) and three minutes post stimulation with laser off. This protocol intended to create a more prolonged/constant physiological firing rate of MSNs.

For LIDs inhibition experiments, two further protocols were used. The first one, using ChR2 (Protocol C), consisted of one minute baseline period, then one minute with continuous blue light stimulation, one-minute post-stimulation period, then one minute with 10 Hz stimulation and one-minute post-stimulation. The second protocol, using eNphR3.0 (Protocol D), consisted of a three-minute baseline period followed by five intervals of 30 s with continuous yellow laser stimulation separated by 30 s without stimulation (Fig. 1A).

2.4. Behaviour

Optodyskinesias (light-evoked dyskinesias) and LIDs were evaluated by placing animals in glass cylinders surrounded by mirrors to facilitate observation of the animal from all directions. During each rating period, individual scores were given for axial, limb and orolingual dyskinesias. Axial dyskinesia consisted of contralateral twisted posturing of the neck and upper body contralateral to the side of the 6-OHDA lesion; forelimb dyskinesias were repetitive jerks or dystonic posturing of the contralateral forelimb; and orolingual dyskinesia included stereotyped jaw

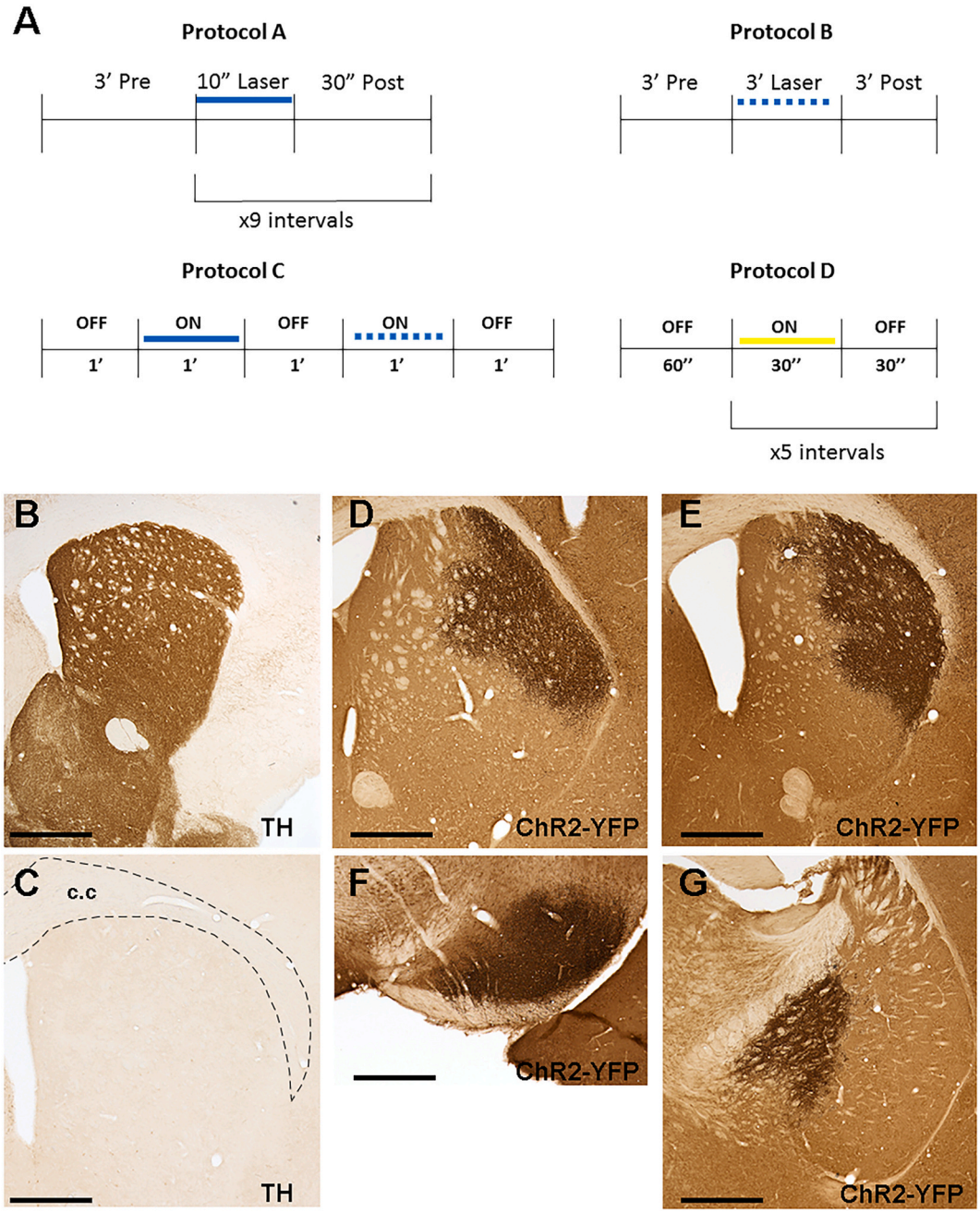

Fig. 1. Image of a coronal slice of a mouse brain showing TH immunoreactivity and Cre-dependent viral expression of ChR2-YFP. **(A)** Optogenetic protocols used in this study. **(B)** TH expression in the ipsilateral striatum to saline/6OHDA injection of sham and dopamine depleted animals. **(C)** Expression in D1-Cre-mice of ChR2-YFP in D1R-expressing neurons in the striatum. **(D)** Expression in A2a-Cre-mice of ChR2-YFP in D2R-expressing neurons in the striatum. **(E)** Axonal projections of ChR2-YFP in D1R-expressing neurons in the Substantia Nigra *pars reticulata*. **(F)** Axonal projections of ChR2-YFP in D2R-expressing neurons in the *Globus Pallidus*. **(G)** Magnification of image 1D showing expression of ChR2-YFP in striatal MSNs Scale bar: 2 mm for image B, 500 μm for images C, D, E, F and 50 μm for image G.

movements, mouth openings and tongue protrusions. Each dyskinetic movement was rated for duration using the following scale: 0 = not present; 1 = dyskinesia present for <50% of the observation time; 2 = dyskinesia present for >50% of the observation time; and 3 = dyskinesia present during the entire observation time. In protocol A, we analyzed each of the 9 stimulation periods as an independent event and computed the sum of the scores for each individual dyskinesia within a given session (3 dyskinesia types x 3 (max score) x 9 times (protocol A) = 81 (maximum score)). In protocol B we analyzed each minute of the stimulation period separately to assess specific changes that happened over time during the session (maximum score per minute = 9). For the LIDs inhibition experiments, optogenetic protocols (protocols C and D) were applied 20, 40 and 60 min after L-DOPA injection to capture the period of peak dose dyskinesias. Net rotational behaviour was calculated by subtracting contralateral rotations to ipsilateral turns, so as negative net rotations mean contralateral bias and positive net rotations mean ipsilateral bias. The threshold to count rotations was 180°

2.5. Drug treatment

Dopamine depleted mice were administered with daily L-DOPA (20 mg/kg, i.p., Sigma-Aldrich) treatment for a week. In one set of experiments, D1-cre animals were tested two days after the L-DOPA treatment to see the effect of L-DOPA priming on optodyskinesias. To test whether

LIDs could be suppressed by selective optogenetic manipulation of each striatal pathways, different acute doses of L-DOPA (6 and 12 mg/kg) were used to induce different levels of dyskinetic behaviour.

L-DOPA was freshly prepared in 0.9% NaCl before used, injected in a volume of 1 ml/kg and was always co-administered with benserazide (benserazide hydrochloride, 10 ml/kg, i.p., Sigma-Aldrich) to block peripheral metabolism to dopamine.

2.6. Brain tissue collection and immunostaining

After completion of experimental testing and 60 min after the last laser stimulation, animals were deeply anesthetized (Sodium pentobarbital, 100 mg/kg) and perfused transcardially with saline (NaCl al 0.9% followed by 4% PFA (PB: 0,1 M; pH 7,3) at a constant rate (10 ml/min). Brains were removed and stored in 30% sucrose solution (PB 0.1 M) until they sank. Coronal sections (30 μm thick) containing the striatum or the substantia nigra were cut in a freezing microtome (Leica Microsystems, Spain). Tissue was stored at 4 °C in a PB solution (0,1 M; pH: 7,3; 0,02% azida) until processed histologically. Immunohistochemistry was performed on free-floating coronal brain sections as described previously (Hernandez et al., 2017). Sections were incubated overnight at 4 °C with the following rabbit antisera: tyrosine hydroxylase (TH, 1:1000, AB152, Millipore, Massachusetts, USA), GFP (1:1000, A-6455, Thermo-Fisher, Massachusetts, USA), cFos (1:1000, ABE457, Millipore, Massachusetts, USA) and FosB (1:7500, sc-48, Santa Cruz Biotechnology, Santa Cruz, USA). Slices were then incubated in secondary antibodies goat anti-rabbit (1:1000, BA-1000, Sigma, Spain) for 1 h at room temperature. Quantification of cFos and FosB positive cells was carried out using Image J (1.42; National Institutes of Health, Bethesda, Maryland). The number of immunolabeled cells were determined for five animals of each group using five serial rostrocaudal sections per animal from both hemispheres. Digital images were taken with a Leica microscope using a 40× magnification. These data are presented as the total number of positive cells per square millimeter in the following three regions of interest: dorsomedial, dorsolateral and ventral striatum. Each region of interest was 73,868 μm^2.

2.7. Extracellular recordings of photoidentified MSNs

To record striatal activity during optogenetic experiments we used a single-drive movable microbundle (sixteen 23-μm tungsten electrodes, Innovative Neurophysiology) coupled to an optic-fiber (230 μm diameter, 0.39 NA, Thorlabs FMT 200 EMT) placed just at the top of the electrode microbundle cannula.

Experiments started ten days after electrode implantation. Neural activity was synchronized with the timestamps from the light stimulation via TTL pulses triggered by a pulse generator (Master 8, AMPI) and recorded using a Cerebus recording system (Blackrock Microsystems).

Putative single units were sorted online using an online sorting algorithm (Central software, Blackrock Microsystems) during the optogenetic protocols. When all protocols were recorded at the same depth, the microbundle was lowered 50 μm to record the next experimental day. The microbundles were moved on average a total of 554 ± 21 μm.

2.8. Spike sorting and cell classification

Units were manually resorted again with an offline sorting algorithm (Offline Sorter V3, Plexon Inc) to isolate single units based on waveform features and inter-spike intervals (ISI). To be classified as a single unit, the following criteria was utilized: (1) percent of ISI violations (<1.2 ms) was <0.1%, (2) the cluster was statistically different ($p < 0.05$) from the other single-units and multi-units in the same wire.

Single units were classified as putative MSNs based on their firing rate, spike waveforms, interspike intervals and peri-event raster plots (Kubota et al., 2009; Hernandez et al., 2013). Only putative MSNs were included in the subsequent analysis.

2.9. Criteria used to photoidentified MSNs

To photoidentify MSNs we delivered a screening protocol consisting of a train of 100 blue light pulses (10 ms width) delivered at 1 Hz. Using neurophysiology data analysis software (Neuroexplorer V4) and Matlab (Mathworks) custom code, we built peri-stimulus time histograms (PSTH) aligned to the light onset in 1 ms bins. PSTH distributions from −900 to −10 was used as baseline activity and compared to a 50 ms window after the laser. A medium spiny neuron was considered photoidentified if it met the following criteria: (1) a significant increase in the firing rate above the 99% confidence interval of baseline activity (>2.56SD) during at least four consecutive bins, (2) the median latency to respond was <10 ms, (3) laser-evoked waveforms were not different from spontaneous waveforms ($R > 0.9$).

2.10. Criteria to identify neurons modulated by laser stimulation

PSTH for each spike trains were generated for the protocol A (width: 14 s, baseline: 2 s, bin size: 100 ms), protocol B (width: 300 s, baseline: 60s, bin size: 1 s) and protocol C (one-minute continuous light, width: 180 s, baseline: 60s, bin size: 1 s). A unit was considered positively modulated by the laser if its firing rate rose above 2SD the mean firing rate of baseline activity for three consecutive bins. A unit was classified as negatively modulated by the light if its firing rate dropped 1SD the mean firing rate of baseline activity for three consecutive bins (baseline activity was often too low to use a mean -2SD criterion). Neurons with baseline firing rate <0.4 Hz were excluded from this analysis.

2.11. Data and statistical analysis

Data exclusion criteria were as follows: in some cases, injection of AAV caused insufficient AAV-dependent ChR2 expression; optogenetic cannula was not correctly placed; and in fewer cases, dopamine depletion was not complete. Exclusions resulted in slightly unbalanced experimental groups. Statistical analyses were performed with GraphPad Prism 6 software (La Jolla, CA). Unless stated otherwise, the data is expressed as the mean ± standard error of the mean (SEM). The minimum significance level was $p \leq 0.05$.

All optogenetic protocols were applied four times for each animal, and the median value individually obtained. Behavioural data comparing sham versus dopamine depleted animals and pre- versus post- L-DOPA treatment were analyzed using a two-way repeated measures ANOVA followed by a Sidak post-hoc test. The analysis of optogenetic experiments trying to inhibit L-DOPA-induced dyskinesias (LIDs) by activating indirect pathway was performed using the Friedman test, followed by Dunn's multiple comparisons test. In protocol D, abnormal involuntary movements were measured during the periods termed 'OFF (1)', 'ON', and 'OFF (2)'. The 'OFF (1)' period was the 30s preceding the laser and the 'OFF (2)' period was the period of 30s after the end of the laser illumination. To compare 'OFF' (1) and 'ON' periods, the Wilcoxon sign-rank test was employed. The analysis of positive FosB cells was done within each group (sham or dopamine depleted) using a two-way repeated measured ANOVA followed by a Sidak post-hoc test.

3. Results

3.1. Validation of the model

To obtain the parkinsonian model, 6-OHDA (saline for the sham control group) was injected into the right MFB. This caused severe depletions of dopamine in the ipsilateral striatum (Fig. 1B). To stimulate the direct and indirect striatal pathways independently, an adeno-associated virus containing ChR2 was injected in the dorsolateral striatum of D1- and A2a-cre mice, respectively. Histological analysis of the expression of ChR2-YFP in D1-Cre (Fig. 1C) or A2a-cre animals (Fig. 1D) in striatal output neurons was confirmed by the selective

presence of ChR2-YFP labeled axon terminals in the substantia nigra *pars reticulata* (SNpr) (Fig. 1E) and globus pallidus (Fig. 1F) and respectively.

3.2. Selective activation of the direct pathway, but not indirect pathway, induced optodyskinesias

We previously reported that simultaneous stimulation of both striatal pathways reproduced abnormal involuntary movements induced by L-DOPA (Hernandez et al., 2017). In the present study we tested whether stimulation of the direct pathway alone was sufficient to induce abnormal involuntary movements. Selective optogenetic D1-R expressing neurons activation produced dyskinesias and contralateral rotations, both in intact (sham control) and dopamine depleted animals (Video S1). These movements resembled those evoked by L-DOPA (Fig. 2A-D) and were elicited by both continuous (Protocol A) (Total score:(main effect/time: $F(2,22) = 34.49$, $P < 0.0001$; main effect/condition: $F(1,11) = 0.237$, $P = 0.636$; interaction effect/time×condition: $F(2,22) = 0.765$, $P = 0.478$) and 10 Hz stimulation protocols (protocol B) (Total score: (main effect/time: $F(4,44) = 65.9$, $P < 0.0001$; main effect/condition: $F(1,11) = 0.288$, $P = 0.603$; interaction effect/time×condition: F(4,44)

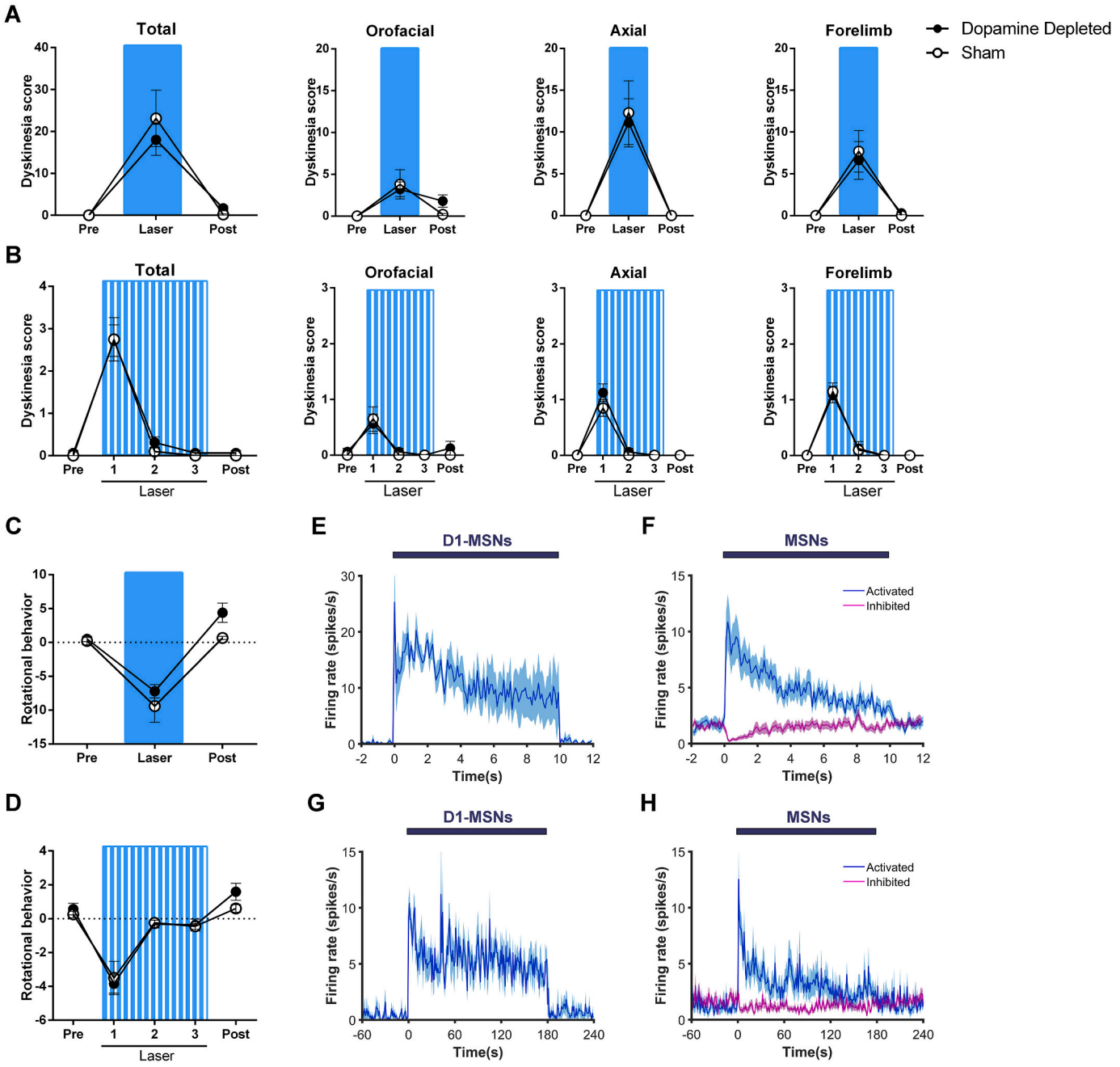

Fig. 2. Selective optogenetic activation of D1R-expreessing neuron elicits dyskinetic behaviour in both DA-depleted and sham animals. **(A, B)** Abnormal involuntary movements for axial, forelimb and orofacial segments before (Pre), during and after (Post) laser stimulation in dopamine depleted ($n = 8$) and sham ($n = 5$) animals with continuous light **(A)** and 10 Hz **(B)**. **(C, D)** Rotational behaviour induced by optogenetic stimulation of D1-MSNs neurons with continuous light protocol **(C)** or 10 Hz **(D)**. **(E, F)** Population peri-stimulus time histograms (PSTHs) for **(E)** photo-identified D1-MSNs ($n = 4$ cells) and **(F)** putative MSNs ($n = 78$ cells, 22 activated and 56 inhibited) in D1-cre mice ($n = 3$ animals) stimulated with 10 s of continuous light. **(G, H)** Population peri-stimulus time histograms (PSTHs) for **(G)** photo-identified D1-MSNs ($n = 5$ cells) and **(H)** putative MSNs ($n = 75$ cells, 17 activated and 58 inhibited) in D1-cre mice (n = 3 animals) stimulated three minutes with 10 Hz. Data shown are means ± SEM.

=0.088, $P = 0.986$). Similar dyskinetic scores were obtained for the different dyskinetic behaviours exhibited by both sham and dopamine depleted animals, with both experimental protocols. The three subtypes of dyskinesia were present in all animals, but with a clear prevalence of axial dystonia. To rule out the possibility that light itself could induce any abnormal behaviour, perhaps due to temperature effects (Owen et al., 2019), same animals were exposed to yellow light (594 nm). The absence of abnormal involuntary movements in this condition confirmed that the observed behavioural effects were due to specific excitatory optogenetic manipulation of the direct pathways caused by the blue light.

To record the activity of D1-MSNs during these optogenetic protocols, we implanted three D1-cre dopamine depleted animals with 16-channel movable electrode bundles coupled to a fiber-optic cannula placed in the dorsolateral striatum. Next, we used a photoidentification protocol (Lima et al., 2009) to identify putative D1-MSNs. This was done by recording neuronal activity during the optogenetic stimulations, where peri-stimulus time histograms (PSTH) were aligned to the laser onset. The application of 10s continuous light induced a strong excitation in all photo-identified D1-MSNs (Fig. 2E); while neighboring MSNs were classified as activated or inhibited by the laser stimulation. The firing rate of the activated MSNs remained increased during the length of the stimuli, whereas the inhibited neurons seemed to be inhibited only during a small period of time (Fig. 2F). Subsequently, we studied the effects of protocol B, since the effects of the stimulation on behaviour only lasted for 20–30 s. Interestingly, although the activity of photo-

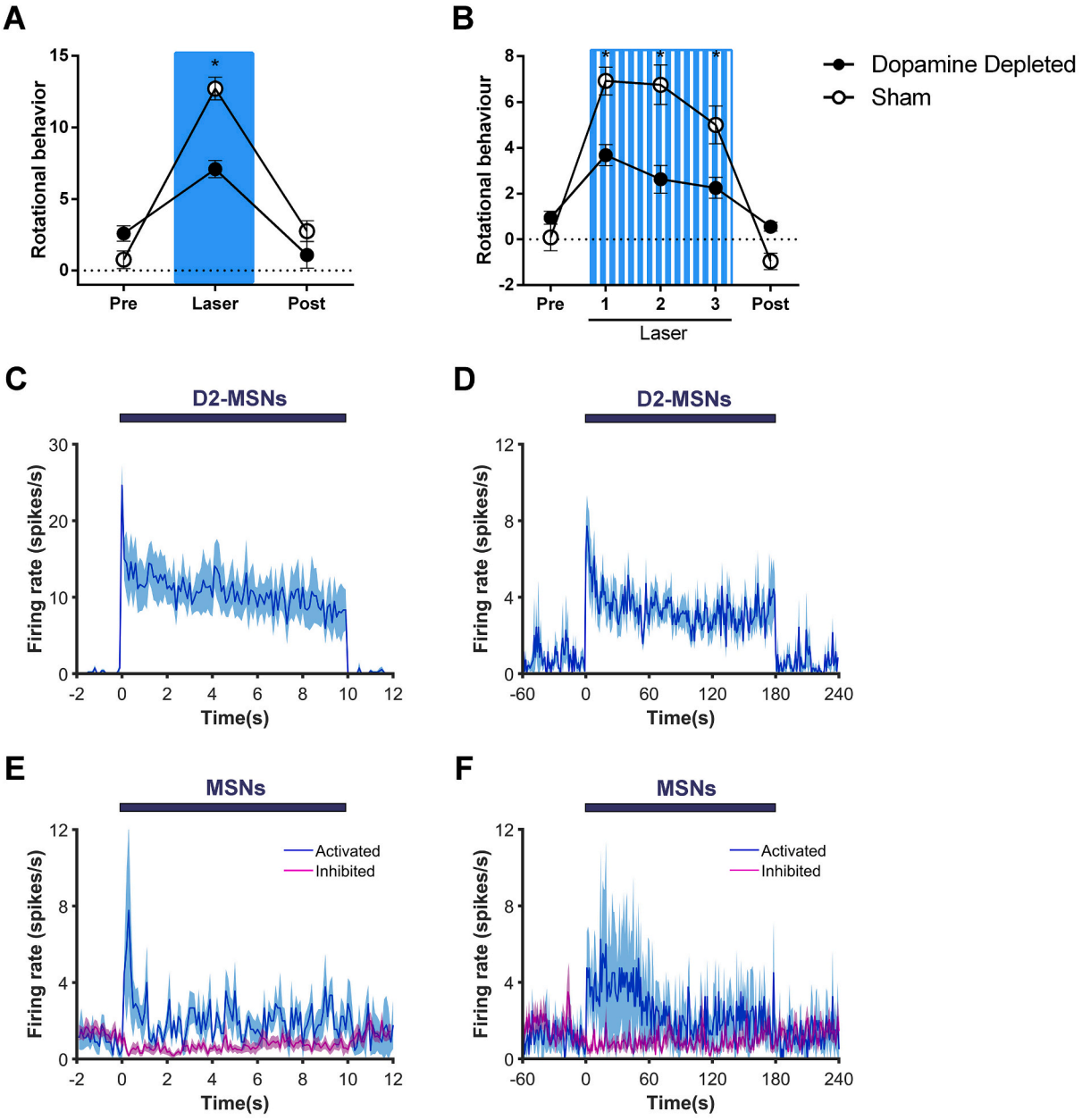

Fig. 3. Selective optogenetic activation of D2R-expressing neurons induced ipsilateral rotations in both DA-depleted and sham animals. **(A, B)** Rotational behaviour induced before (Pre), during and after (post) laser stimulation of D2R-expressing neurons with continuous light **(A)** and 10 Hz **(B)** in dopamine depleted ($n = 9$) and sham ($n = 6$) A2a-cre animals. **(C, D)** Population peri-stimulus time histograms (PSTHs) for photo-identified D2-MSNs in A2a-Cre mice (n = 3 animals) stimulated **(C)** with continuous light (n = 6 cells) and **(D)** three minutes with 10 Hz. (n = 7 cells). **(E, F)** Population peri-stimulus time histograms (PSTHs) for putative MSNs in A2a-Cre mice (n = 3 animals) stimulated **(E)** with continuous light ($n = 29$ cells, 5 activated and 24 inhibited) and **(F)** three minutes with 10 Hz. ($n = 30$ cells, 4 activated and 26 inhibited) **(F)**. Data shown are means ± SEM. *$p < 0.05$, significantly different between groups, two-way ANOVA repeated measures, Sidak post hoc test.

identified D1-MSNs (Fig. 2G) was increased throughout the three-minute 10 Hz stimulation protocol, the dyskinesias induced by the stimulation were only present during the first minute of stimulation (Fig. 2B, D). This effect could be due to changes in the activity of downstream basal ganglia nuclei operating to compensate for the increased activity of the D1-MSNs. Regarding the neighboring MSNs, as happened with continuous light, the activated MSNs showed a sharp increase in firing rate that declined over time, whereas the effect on inhibited cells was more nuanced. (Fig. 2H).

Selective activation of the indirect pathway in the A2a-cre mice caused ipsilateral turning with both experimental protocols (Fig. 3A-B), (Continuous light: main effect/time: $F(2,26) = 104.9$, $P < 0.001$; main effect/condition: $F(1,13) = 5.999$, $P = 0.00$; interaction effect/time×condition: $F(2,26) = 16.67$, $P < 0.001$) which was continuously present during the three-minute 10 Hz protocol (Fig. 3B, 10 Hz: main effect/time: $F(4,52) = 83.37$, $P < 0.001$;main effect/condition: $F(1,13) = 7.228$, $P = 0.001$; interaction effect/time×condition: $F(4,52) = 22.02$, $P < 0.001$). Surprisingly, the optogenetic stimulation produced more frequent ipsilateral rotations in intact than in dopamine depleted animals ($p < 0.05$, Sidak's post-hoc test). Apart from such ipsilateral circling, no abnormal movements were elicited by indirect pathway stimulation in either the dopamine depleted or the sham animals.

In these A2a-cre animals, the stimulation with both protocols also induced strong activation of D2-MSNs neurons that lasted the whole length of the stimuli (Fig. 3C-D). Regarding the changes in neighboring MSNs, both protocols induced a transient increased in firing rate in the MSNs that were activated by the laser, whereas the ones inhibited showed an inhibition for almost all the length of the stimuli (Fig. 3E-F).

Contrary to D1-MSNs stimulation, the behavioural effects of D2-MSNs activation lasted throughout the 3 min of laser stimulation, and this could be due to the activation of non-identified MSNs that have an effect on the behavioural output.

3.3. L-DOPA priming potentiates optodyskinesias

To test how optically induced dyskinesias might be influenced by prior L-DOPA treatment, we administered the drug daily (20 mg/kg, i.p.) in dopamine depleted animals that had previously demonstrated optodyskinesias with the laser. Two days after the last L-DOPA injection, these L-DOPA primed animals were optically stimulated. Compared with the optodyskinesias obtained before L-DOPA treatment, selective optical activation of the direct pathway induced significantly higher dyskinesia scores during the light ON (Fig. 4A, main effect/time: $F(2,14) = 40.33$, $P < 0.001$; main effect/condition: $F(1,7) = 10.27$, $P = 0.0150$; interaction effect/time×condition: $F(2,14) = 10.45$, $P = 0.002$). This suggests that L-DOPA treatment primes the system, making it more sensitive to the same optogenetic stimulus and exhibiting a higher dyskinetic score after L-DOPA exposure. This potentiation effect on dyskinesias was not observed during protocol B (Fig. 4B, main effect/time: $F(4,56) = 82.44$, $P < 0.001$; main effect/condition: $F(1,14) = 1.570$, $P = 0.2308$; interaction effect/time×condition: $F(4,56) = 0.423$, $P = 0.7615$). Interestingly, L-DOPA administration increased contralateral rotations in these animals with both continuous light (Fig. 4C,main effect/time: $F(2, 14) = 34.46$, $P < 0.001$; main effect/condition: $F(1,7) = 3.739$, $P = 0.094$;

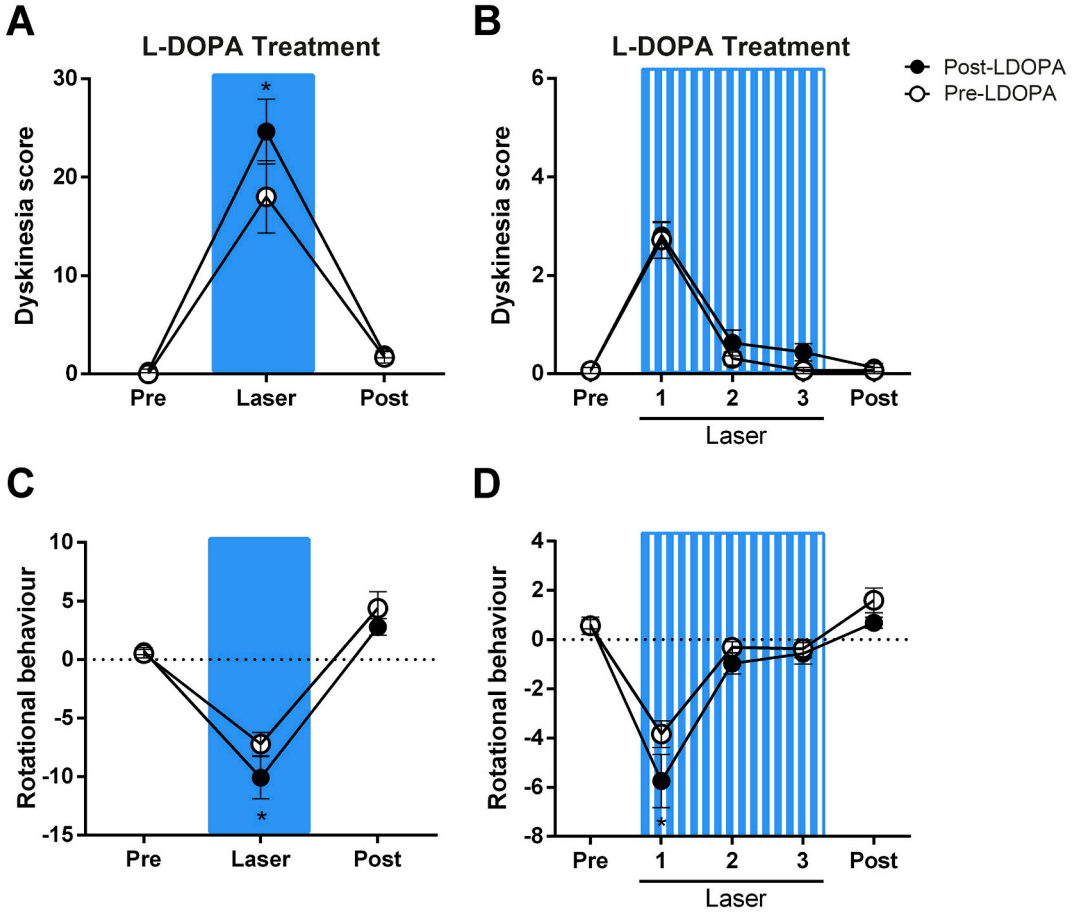

Fig. 4. L-DOPA treatment potentiates optodyskinesias. **(A, B)** Comparison between the dyskinetic effects of selective D1-MSNs activation in dopamine depleted animals (n = 8 animals) before and after L-DOPA treatment with continuous light **(A)** and 10 Hz **(B)**. **(C, D)** Comparison of the rotational behaviour induced by stimulation of D1-MSNs in dopamine depleted animals (n = 8 animals) before and after L-DOPA treatment with continuous light **(C)** and 10 Hz **(D)**. Data shown are means ± SEM. *p < 0.05, significantly different between groups, two-way ANOVA repeated measures, Sidak post hoc test.

interaction effect/time×condition: F(2,14) = 4.321, $P = 0.035$), and the 10 Hz frequency protocols (Fig. 4D,main effect/time: F(4, 28) = 32.62, P < 0.001; main effect/condition: F(1,7) = 2.435, $P = 0.163$; interaction effect/time×condition: F(4,28) = 3.604, $P = 0.017$). These results suggest that rotational behaviour and dyskinesia maybe mediated by different mechanisms.

3.4. Optogenetic inhibition of levodopa-induced dyskinesias

Recently, it was reported that during LIDs there is unbalanced activity between the direct and indirect striatal pathways (Parker et al., 2018; Ryan et al., 2018). The activity of the direct pathway neurons during LIDs was two times the activity seen in normal conditions, while the activity of the indirect pathway was below control levels (Ryan et al., 2018). We therefore tested whether LIDs could be suppressed by restoring a balance of activity between the direct and indirect pathways.

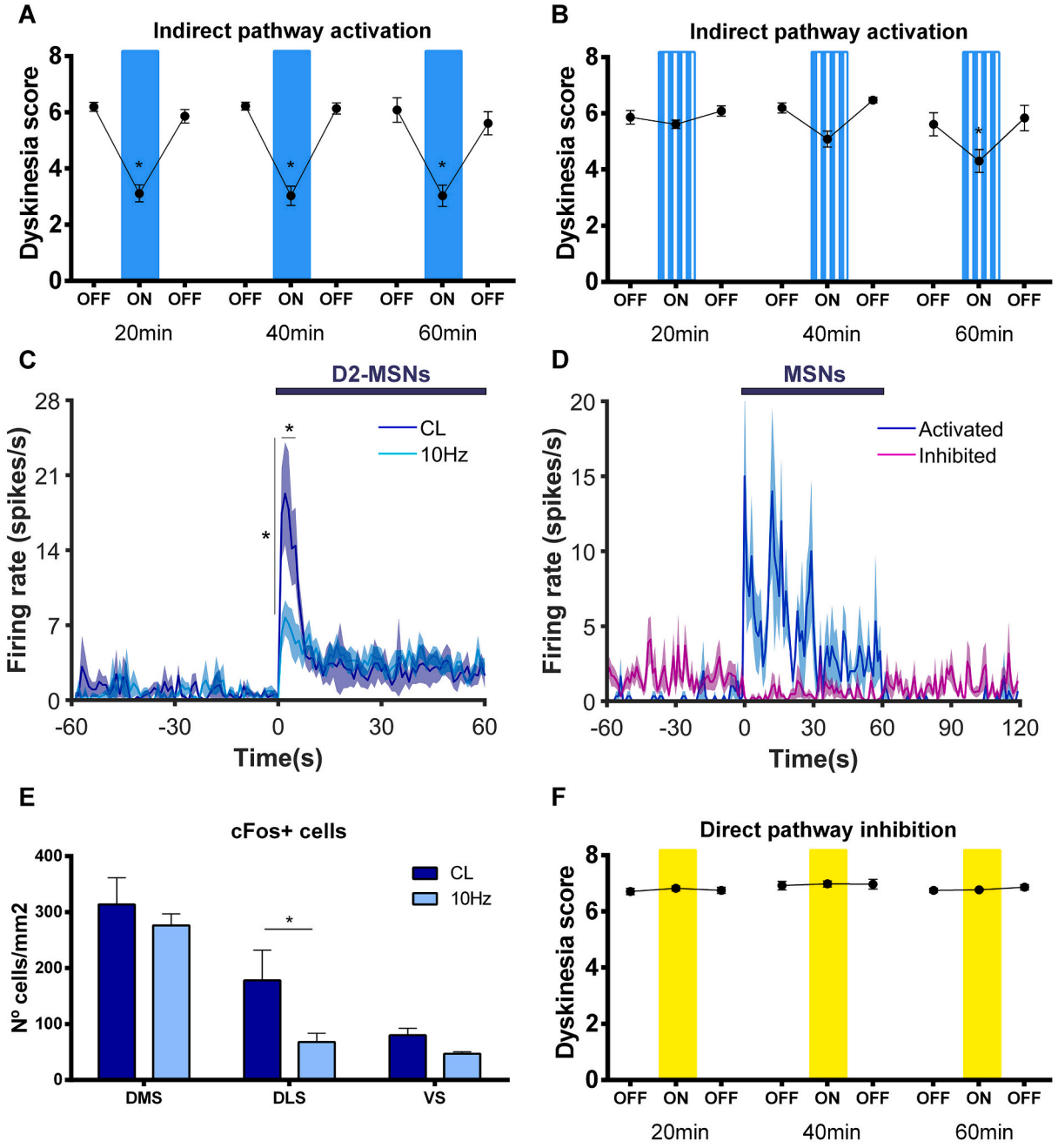

Fig. 5. Optogenetic activation of indirect pathways successfully reduced LIDs. **(A)** Activation of indirect pathway with continuous light blocks LIDs at the 3 different time-points. Data shown are means ± SEM from n = 9 A2a-cre mice. **(B)** Activation of indirect pathway with 10 Hz protocol only reduces LIDs at the 60 min time-point. Data shown are means ± SEM from n = 9 A2a-cre mice. **(C)** Comparison of firing rate for A2a-photoidentified cells during the one-minute continuous light (n = 7 cells) and 10 Hz (n = 7 cells) stimulations protocols. Data shown are means ± SEM. *p < 0.05, significantly different between protocols for the first 5 s, two-way ANOVA repeated measures, Sidak post hoc test. **(D)** Activity of putative MSNs activated (n = 3) and inhibited ($n = 21$) during the one-minute continuous light protocol. **(E)** Histogram represents quantification of cFos-positive cells in A2a-cre mice sacrificed after continuous light (n = 4 animals) and after 10 Hz (n = 5 animals) stimulations protocols. DMS (Dorsomedial striatum), DLS (Dorsolateral striatum), VS (Ventral striatum). **(F)** Inhibition of striatal direct pathway failed to reduce LIDs at the different time points. Data shown are means ± SEM from n = 5 mice.

To do so, we tried two different approaches.

We first attempted to increase the reduced activity of the indirect pathway during LIDs. To do that, nine 6-OHDA-treated A2a-cre animals received L-DOPA treatment daily (20 mg/kg) for five days to make them dyskinetic. Two days after last L-DOPA injection, animals were challenged with 12 mg/kg of L-DOPA. While animals were exhibiting classical LIDs, optogenetic stimulation of D2-MSNs was applied 20, 40 and 60 min after the L-DOPA injection. Optically induced activation of the indirect pathway with continuous light caused a two-fold reduction in the LIDs scores at each of the three time points (Fig. 5A, OFF (1) vs. ON, 20 min $p < 0.05$; 40 min, $p < 0.05$; 60 min, $p < 0.05$, Dunn's multiple comparison test). Optogenetic stimulation with 10 Hz light reduced LIDs only at 60 min post L-DOPA injection (Fig. 5B, OFF (1) vs. ON, 60 min, $p < 0.05$). This suppressive effect on LIDs was achieved without rendering the animal akinetic/immobile. Indeed, the reduced levels of dyskinesia were replaced by seemingly normal exploratory behaviour (VideoS3). To reveal the physiological effects of the optogenetic stimulation, we recorded the activity of D2-MSNs during the different light protocols (one minute of continuous light and one-minute 10 Hz stimulation. Comparing the activity induced by both protocols, we found that continuous light induced significantly more D2-MSN activity than 10 Hz stimulation during the first five seconds of the stimulation (Fig. 5C,: main effect/time: $F(119, 1428) = 8.560$, $P < 0.001$; main effect/condition: $F(1,12) = 0.063$, $P = 0.806$; interaction effect/time×condition: $F(119, 1428) = 2.069$, $P < 0.001$)). Also, when looking at the effects produced by 1 min of continuous light in the surrounding neurons, we found that inhibited neurons were inhibited during the whole period of stimulation, whereas the activated neurons had higher firing rates mainly during the first half of the minute (Fig. 5D). To further assess the activity levels of MSN neurons, we sacrificed animals 60 min after protocols A ($n = 5$) and B ($n = 4$) and measured the striatal expression of cFos. Significantly more cFos+ cells were found in the dorsolateral striatum induced by protocol A than protocol B (Fig. 5E: main effect/time: $F(2,21) = 34.59$, $P < 0.001$; main effect/condition: $F(1,21) = 6.494$, $P = 0.0187$; interaction effect/time×condition: $F(2, 21) = 1.122$, $P = 0.345$). These results are consistent with the electrophysiological finding that continuous light recruits (stimulates) a higher number of D2-MSNs than 10 Hz stimulation. To rule out the possibility that the anti-dyskinetic effect of this manipulation was due to changes in temperature, pH or other unspecific effects (Owen et al., 2019) same animals were illuminated with yellow light (594 nm), showing no change in behaviour, and demonstrating that the behavioural effects obtained were due to the selective activation of the indirect pathway obtained with the blue light (473 nm) (Video S2).

In a second approach, we attempted to reduce the activity of the direct pathway during LIDs. To do that, we injected the inhibitory halorhodopsin eNpHR3.0 in D1R-expressing neurons of 6-OHDA treated D1-cre mice (Supplementary Fig. 1). Four weeks after the surgery, and bearing in mind that inhibitory opsins are less efficient than excitatory ones (Han, 2012), animals were directly challenged with 6 mg/kg of L-DOPA. At 20, 40 and 60 min after L-DOPA injection, while animals were exhibiting LIDs, we applied a protocol of continuous light to reduce the activity of the direct pathway. Somewhat unexpectedly, selective inhibition of these neurons failed to have any behavioural effect on L-DOPA-evoked dyskinesias (Fig. 5E and Video 3).

3.5. Selective direct pathway activation increased dyskinesia-related molecular markers only in dopamine depleted animals

FosB is an established molecular marker that is expressed in the striatum selectively for dyskinesia (Cenci et al., 1999; Pavón et al., 2006). We therefore analyzed whether selective stimulation of the direct pathway was sufficient to induce FosB expression. This explored further our previous report that striatal FosB was expressed after opto-dyskinesias evoked by combined stimulation of both striatal pathways in rats (Hernandez et al., 2017). Consequently, animals were sacrificed 60 min after the last Protocol A experiment. Compared to the contralateral side, selective activation of the direct pathway increased the expression of FosB in dorsomedial (DMS) and ventral striatum (VS) (Fig. 6A, B; Dopamine depleted (main effect/area: $F(2,24) = 4.260$, $P = 0.0261$; main effect/hemisphere: $F(1,24) = 22.13$, $P < 0.001$; interaction effect/area×hemisphere: $F(2,24) = 3.745$, $P = 0.0384$; Sham: (main effect/area: $F(2,24) = 3.106$, $P = 0.063$; main effect/hemisphere: $F(1,24) = 0.006$, $P = 0.936$; interaction effect/area×hemisphere: $F(2,24) = 0.305$, $P = 0.740$; two-way repeated-measures ANOVA), but only in dopamine depleted animals. In sham control animals, despite exhibiting behavioural optodyskinesias, FosB expression levels were not significantly increased. This finding supports previous results indicating that this immediate early gene can act as a molecular marker for dyskinesias, but only in dopamine deprived preparations (Cenci et al., 1999; Pavón et al., 2006).

These results show that optogenetically induced dyskinetic movements have the same molecular correlate described for the traditional LIDs, thereby extending the reach of this approach in the study of dyskinesia.

4. Discussion

The main finding of the current study was that selective optogenetic activation of indirect pathway caused a reduction in the expression of LIDs. We also observed that selective activation of direct pathway provoked behavioural dyskinesias and that this effect was enhanced by priming with systemic L-DOPA.

The former result fits well with the traditional movement inhibition role attributed to the indirect efferent circuit of the striatum (Kravitz et al., 2010; Freeze et al., 2013). But it could also be explained by the fact that D2R-expressing neurons could be inhibiting activity associated with unwanted movements (Mink, 1996). In fact, PD patients with dyskinesias worsen their motor performance when trying to make voluntary movements. LIDs in animal models have been associated with an activity imbalance between the two efferent striatal pathways. During LIDs, activity levels in direct pathway was almost doubled, and activity in indirect pathway was reduced (Ryan et al., 2018). Treatments to increase D2-MSNs activity would therefore be expected to produce a more normal balance between the direct and indirect projections and these results, contribute to highlight the relevance of an adequate activity balance between the direct and indirect pathways in both physiological and pathological conditions. Therefore, these results seem to indicate that D2-MSN activation suppresses dyskinesia not only by activation of the indirect pathway, but also by inhibiting or outcompeting D1-MSN activity, possibly by intrastriatal lateral inhibition (Taverna et al., 2008). It is the combination of the two events that leads to suppression of abnormal involuntary movements, since inhibiting D1-MSN alone fails to produce the same effect. Studies using Designer Receptors Exclusively Activated by Designer Drugs (DREADDs) (Alcacer et al., 2017) support this view. Importantly, in the present study, the anti-dyskinetic effect of D2-MSNs stimulation occurred while animals were engaged in apparently normal unforced behaviour, e.g. periodic exploration. During the laser stimulation there was no evidence of incompatible behaviours such as freezing. This has been a traditional problem with most therapeutic interventions designed to manage LIDs in PD patients. In our experiments, continuous light was more efficient than 10 Hz stimulation in suppressing LIDs. Additionally, with both electrophysiological and immunochemical procedures we showed continuous light stimulation was more effective at recruiting a larger population of neurons with increased levels of firing activity and cFos expression, thereby allowing for the suppression of the dyskinetic behaviour induced by LDOPA (Fig. 5C, E and (Jáidar et al., 2019)).

Confirming the finding of another group (Girasole et al., 2018), D1-MSNs inhibition in our hands did not modify LIDs expression. This differs from the previous studies that used different animal models to show LIDs were associated with an aberrant increase in D1R-signaling (Cenci

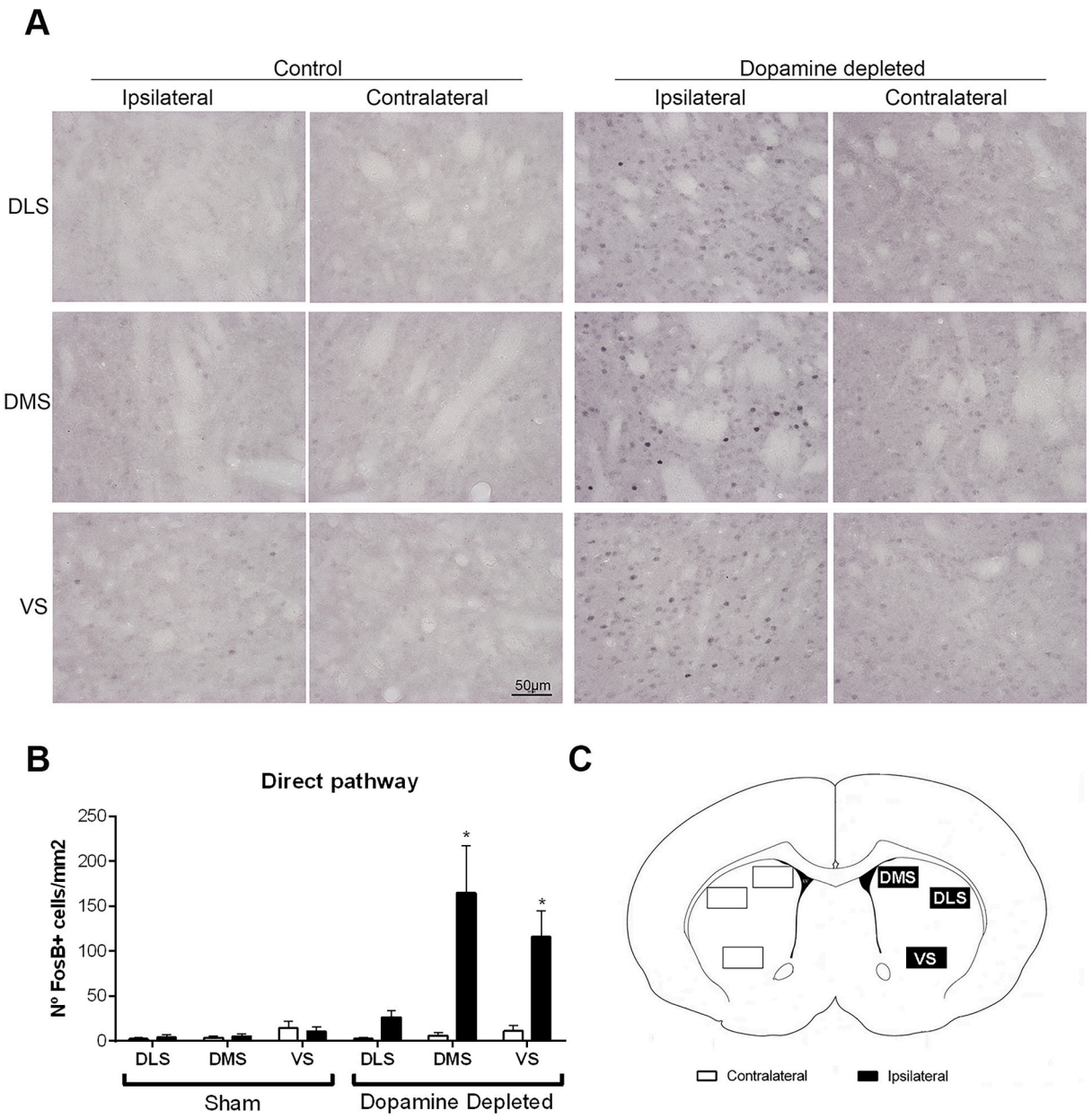

Fig. 6. Optogenetic activation of D1-MSNs in the striatum induced FosB expression only in dopamine-depleted animals. **(A)** Immunochemistry images showing FosB staining in the ipsilateral and contralateral side of stimulation in sham (n = 5) and dopamine depleted (n = 5) animals. **(B)** Histogram represents quantification of FosB+ cells. **(C)** Diagram showing the areas of quantification from the Paxinos and Franklin brain atlas (2001). Data shown are means ± SEM. *p < 0.05, significantly different between hemispheres, two-way ANOVA repeated measures, Sidak post hoc test.

and Konradi, 2010; Heumann et al., 2014). The finding is also at variance with the reports of anti-dyskinetic effects after deleting D1R or DARPP-32 proteins in direct pathway neurons (Darmopil et al., 2009; Bateup et al., 2010) or the recently published work by Gao and colleges (Gao et al., 2022) where optogenetic inhibition of D1-MSNs causes reduction in LIDs behaviour in rats. There may be several reasons for these discrepancies. Firstly, regarding Gao et al. (2022), the use of a different animal model may be the cause of this disparity in results. We have shown in the past how optogenetic stimulation in intact rats do not cause LIDs (Hernandez et al., 2017), while it evokes dyskinesia in control mice. When comparing with the systemic treatments used before, our laser inhibition would have had a local regional effect limited to one hemisphere. L-DOPA, on the other hand, will have a broad spectrum of bilateral action throughout the whole brain. However, it should be noted that this regionally limited impact of optogenetic manipulation was not an issue for the selective activation of D2-MSNs that successfully suppressed LIDs. This suggests LIDs may be particularly sensitive to indirect pathway activation compared with direct pathway inhibition. Differential patterns of intrinsic circuitry both in the striatum and efferent structures might explain this difference (Bolam et al., 2000). In fact, D2-MSNs activation indirectly engages a population of arkypallidal neurons in the GP. This effect is thought to have a role in stopping ongoing actions (Mallet et al., 2016; Aristieta et al., 2021). Consequently, we hypothesize that optogenetic activation of D2-MSNs could recruit this pallidal subpopulation, which may in turn be responsible for terminating the L-DOPA-evoked abnormal movements. Methodological differences may also play a role. For example, channelrhodopsins seem to be more efficient at stimulating neuronal activity than halorhodopsins are inhibiting it (Han, 2012). Our results are, however, in agreement with a study that reported no change in dyskinesia after selectively inhibiting

the direct pathway, compared with one when all the striatal neuronal sub-types engaged in dyskinesia were inhibited (Girasole et al., 2018).

Finally, and admittedly somehow theoretical, a pathophysiological puzzle of LIDs (both in rat and monkey model) has classically been that markers of D2-MSNs neuronal activity and indirect striato-pallidal projection remain elevated in the presence of LIDs and levodopa treatment. This is an oddity that was probably artifactually related with the pharmacological L-DOPA regimen administered to cause LIDs and the short plasma half -life of levodopa. In other words, by the time animals were sacrificed, the impact of levodopa was vanished and the brain was returning to the parkinsonian state. To explain this paradox a few explanations were advanced at the time (Obeso et al., 2000; Brotchie et al., 2005) but none was convincing enough. The results here clearly show that activating the indirect pathway is positive and probably achieves a new balance between direct-indirect striatal projections. So, we can conclude that the present work demonstrates that focused stimulation of the indirect pathway effectively suppressed the expression of unwanted LIDs.

The other main result of the current study was that selective activation of D1-MSNs was sufficient to induce optodyskinesias in both dopamine depleted and sham animals. These findings confirm previous studies using either optogenetics (Perez X et al., 2017; Ryan et al., 2018; Keifman et al., 2019) or chemogenetics (Alcacer et al., 2017) in dopamine depleted preparations. Our observation of optodyskinesias in non-dopamine-depleted animals is in agreement with similar reports (Rothwell et al., 2015; Ryan et al., 2018). Interestingly, a previous study using DREADDs in mice was unable to induce dyskinesias in sham group (Alcacer et al., 2017). However, it should be noted that DREADDs and optogenetics have different mechanisms of action. Action potentials are evoked by optogenetic stimulation irrespective of a neurones afferent input. DREADDs on the other hand increase the response of the neurons to incoming excitatory inputs, but it does not alone produce neuronal firing (Alcacer et al., 2017).

Additionally, D2-MSNs stimulation causes rotational behaviour that is significantly different between dopamine depleted and control mice, while D1-MSNs stimulation does not elicit any differences between both groups. This highlights the difference in sensitivity between both pathways to elicit rotational behaviour to dopamine content. Activation of D1- and D2-MSNs will operate through different downstream pathways to produce differences in observed motor behaviours. D2-MSNs stimulation caused rotational behaviour that was significantly different between dopamine depleted and control mice. On the other hand, the rotational behaviour evoked by D1-MSNs stimulation was not reliably different between the depleted and control animals. This emphasises the point that dopamine content is a critical factor for observing rotational behaviour following D1 or D2 stimulation.

LIDs in PD are thought to result from non-physiological activation of super-sensitized dopamine receptors consequent upon severe nigrostriatal degeneration (Picconi et al., 2018). Modern analyses suggest that this aberrant stimulation makes D1-MSNs additionally hypersensitive to their afferent inputs (Fieblinger et al., 2014). Thus, chronic administration of L-DOPA and other dopaminergic agonists that are capable of inducing dyskinesia (Engber et al., 1993) increase signaling in D1-MSNs and suppress activity in D2-MSNs. This in turn causes an abnormal imbalance in the activity levels between the direct and indirect pathways. Consequently, any manipulation that produces an imbalance between both striatal pathways might be expected to produce dyskinesia. However, in PD patients, for such an imbalance to be produced with pharmacological treatment, severe dopamine depletion is required. Nevertheless, imbalance between two striatal projections may be achieved pharmacologically even in the presence of an intact nigrostriatal pathway. Supporting this view are some anecdotal descriptions of dopamine associated dyskinesia-like behaviours present in non-depleted primates, including humans. Thus, dyskinesias were seen in healthy primates following high doses of L-DOPA (twice daily regimen (Togasaki et al., 2001) or nomifensine (a DAT inhibitor) (Togasaki et al., 2005), in patients ($n = 6$) with TH-deficiency (Pons et al., 2013), and in a patient with normal DA striatal levels but with vascular parkinsonism (Quinn et al., 1986).

It is also worth commenting on our observation that the behavioural effects of selective optogenetic activation did not correlate well with the patterns of neuronal activation found in our neuronal recordings. For example, the activity of photo-identified D1-MSNs was elevated throughout the three-minute period of 10 Hz stimulation yet changes in behaviour lasted little less than the first minute of stimulation. Apparently, this is not the case for LIDs, where D1-MSNs activity is more directly correlated with abnormal involuntary movements (Ryan et al., 2018). Perhaps in the case of D1-MSNs optogenetic stimulation some extra-striatal adaptative mechanisms come into play with admittedly, an unusual pattern of imposed neural activation. Moreover, it is also noteworthy that optogenetic stimulation of D1 MSNS induces activation and inhibition of neighboring MSNs, that cannot be identified as D1 or D2-type, but are probably involved and contributing to the behavioural expression observed. On the other hand, selective activation of the indirect pathway by 10 Hz stimulation caused ipsilateral turning throughout the 3 min stimulation period and was accompanied by a maintained increased D2-MSN neuronal activity. This is further evidence that the dynamic patterns of responding to imposed optogenetic stimulation are rather different for direct and indirect pathway MSNs.

There have been several reports that in L-DOPA-primed animals, optogenetic activation of D1R-expressing MSNs or their terminals in the SN that increases the expression of dyskinesia compared with non-primed testing conditions (Perez X et al., 2017; Ryan et al., 2018; Keifman et al., 2019). This supports the view that chronic L-DOPA potentiates the response of basal ganglia circuitry to experimental treatments that activate D1-MSNs. Our finding that FosB expression was increased only in the dopamine depleted animals that exhibited optodyskinesia provides further support to this notion and extends previous work by validating the expression of FosB as a selective marker for dyskinesia in dopamine depleted preparations (Pavón et al., 2006).

In conclusion, the enhanced suppressive effect of indirect pathway activation on LIDs described here suggests that therapeutic tools designed specifically to activate the striatal indirect projection would be expected to block LIDs in PD patients.

5. Conclusions

The present results further confirm previous studies showing that activation of D1-MSNs is enough and sufficient to induce dyskinesia-like movements in the 6-OHDA mouse model of Parkinson's disease. However, it also shows a functional dissociation between striatal pathways and highlights the role of the indirect pathway in dyskinesia since activation of D2-MSNs is enough to inhibit LIDs. Both findings support the notion that the activity of both striatal pathways should be balanced and tightly regulated in order to perform appropriate movements, and despite the majority of the work in the field is focused on the role of direct pathway in dyskinesia, is the indirect pathway the potential therapeutic target to abolish that disabling behaviour. The clinical implications of the findings presented here can only be a matter of speculation. Thus, the suggestion of selective activation of D-2 MSNs pharmacologically is a logical one but unlikely to achieve in practice. On the other hand, the possibility of acting locally at the putamen from an external source by using physical means such as ultrasound to achieve neuroplastic changes is more within the scope of mid-term future developments. In this sense, the current results may be very useful by pointing out an anatomical target, although how to discriminate the effect specifically on the indirect pathway will be challenging.

Supplementary data to this article can be found online at https://doi.org/10.1016/j.nbd.2022.105930.

Funding sources

This work was supported by: Marie Slodowksa-Curie Fellowship, H2020-MSCA-IF-2014_RI:660964-ROSNPD (LFH); and by grants from the Spanish Government: SAF2015–67239-P (JAO), BES-2016-077493 (ICM); CIBERNED (JAO, LFH). Fundación Gangoiti (YVW).

Funding agencies: Marie Slodowksa-Curie Fellowship, H2020-MSCA-IF-2014_RI:660964-ROSNPD (LFH); and by grants from the Spanish Government: SAF2015–67239-P (JAO), BES-2016-077493 (ICM); CIBERNED (JAO, LFH). Fundación Gangoiti (YVW) and by grants PID2019-111693RB-100 funded by MICIN /AEI/http://dx.doi.org/10.13039/501100011033, by European Union's Horizon 2020 research and innovation program, AND-PD (grant agreement no. 84800), and by NextGenerationEU/PRTR (MICIN/CSIC/PTI+ Neuro-Aging) to R.M.

CRediT authorship contribution statement

Iván Castela: Formal analysis, Investigation, Data curation, Writing – review & editing, Funding acquisition. **Raquel Casado-Polanco:** Investigation. **Yaiza Van-Waes Rubio:** Investigation. **Joaquim Alves da Silva:** Methodology, Data curation, Writing – review & editing. **Raquel Marquez:** Investigation. **Beatriz Pro:** Investigation. **Rosario Moratalla:** Resources, Writing – review & editing. **Peter Redgrave:** Writing – review & editing. **Rui M. Costa:** Methodology, Resources, Writing – review & editing, Funding acquisition. **José Obeso:** Resources, Writing – review & editing, Visualization, Funding acquisition. **Ledia F. Hernandez:** Conceptualization, Methodology, Formal analysis, Investigation, Writing – original draft, Visualization, Supervision, Funding acquisition.

Data availability

Data will be made available on request.

Acknowledgements

Authors want to thank José Obeso's lab members and Rui Costa team for experimental support and discussions of the results obtained in this manuscript.

References

Albin, R.L., Young, A.B., Penney, J.B., 1989. The functional anatomy of basal ganglia disorders. Trends Neurosci. 12, 366–375.
Alcacer, C., Andreoli, L., Sebastianutto, I., Jakobsson, J., Fieblinger, T., Cenci, M.A., 2017. Chemogenetic stimulation of striatal projection neurons modulates responses to Parkinson's disease therapy. J. Clin. Invest. 127, 720–734.
Aristieta, A., Barresi, M., Azizpour Lindi, S., Barrière, G., Courtand, G., de la Crompe, B., Guilhemsang, L., Gauthier, S., Fioramonti, S., Baufreton, J., Mallet, N.P., 2021. A Disynaptic circuit in the Globus pallidus controls locomotion inhibition. Curr. Biol. 31, 707–721.e7.
Bateup, H.S., Santini, E., Shen, W., Birnbaum, S., Valjent, E., Surmeier, D.J., Fisone, G., Nestler, E.J., Greengard, P., 2010. Distinct subclasses of medium spiny neurons differentially regulate striatal motor behaviors. Proc. Natl. Acad. Sci. U. S. A. 107, 14845–14850.
Bolam, J.P., Hanley, J.J., Booth, P.A., Bevan, M.D., 2000. Synaptic organisation of the basal ganglia. J. Anat. 196 (Pt 4), 527–542.
Brotchie, J.M., Lee, J., Venderova, K., 2005. Levodopa-induced dyskinesia in Parkinson's disease. J. Neural Transm. 112, 359–391.
Cenci, M.A., 2007. Dopamine dysregulation of movement control in L-DOPA-induced dyskinesia. Trends Neurosci. 30, 236–243.
Cenci, M.A., Konradi, C., 2010. Maladaptive striatal plasticity in L-DOPA-induced dyskinesia. Prog. Brain Res. 183, 209–233.
Cenci, M.A., Tranberg, A., Andersson, M., Hilbertson, A., 1999. Changes in the regional and compartmental distribution of FosB- and JunB-like immunoreactivity induced in the dopamine-denervated rat striatum by acute or chronic L-dopa treatment. Neuroscience 94, 515–527.
Cui, G., Jun, S.B., Jin, X., Pham, M.D., Vogel, S.S., Lovinger, D.M., Costa, R.M., 2013. Concurrent activation of striatal direct and indirect pathways during action initiation. Nature 494, 238–242.
Darmopil, S., Martín, A.B., De Diego, I.R., Ares, S., Moratalla, R., 2009. Genetic inactivation of dopamine D1 but not D2 receptors inhibits L-DOPA-induced dyskinesia and histone activation. Biol. Psychiatry 66, 603–613.
Engber, T.M., Marin, C., Susel, Z., Chase, T.N., 1993. Differential effects of chronic dopamine D1 and D2 receptor agonists on rotational behavior and dopamine receptor binding. Eur. J. Pharmacol. 236, 385–393.
Espay, A., Morgante, F., Merola, A., Fasano, A., Marsili, L., Fox, S., Bezard, E., Picconi, B., Calabresi, P., Lang, A., 2018. Levodopa-induced dyskinesia in Parkinson disease: current and evolving concepts. Ann. Neurol. 84, 797–811.
Fieblinger, T., Graves, S.M., Sebel, L.E., Alcacer, C., Plotkin, J.L., Gertler, T.S., Chan, C.S., Heiman, M., Greengard, P., Cenci, M.A., Surmeier, D.J., 2014. Cell type-specific plasticity of striatal projection neurons in parkinsonism and L-DOPA-induced dyskinesia. Nat. Commun. 5, 5316.
Francardo, V., Recchia, A., Popovic, N., Andersson, D., Nissbrandt, H., Cenci, C., 2011. Impact of the lesion procedure on the profiles of motor impairment and molecular responsiveness to L-DOPA in the 6-hydroxydopamine mouse model of Parkinson's disease. Neurobiol. Dis. 42, 327–340.
Freeze, B.S., Kravitz, A.V., Hammack, N., Berke, J.D., Kreitzer, A.C., 2013. Control of basal ganglia output by direct and indirect pathway projection neurons. J. Neurosci. 33, 18531–18539.
Gao, S., Gao, R., Yao, L., Feng, J., Liu, W., Zhou, Y., Zhang, Q., Wang, Y., Liu, J., 2022. Striatal D1 Dopamine Neuronal Population Dynamics in a Rat Model of Levodopa-Induced Dyskinesia. Front. Aging Neurosci. 14.
Girasole, A.E., Lum, M.Y., Nathaniel, D., Bair-Marshall, C.J., Guenthner, C.J., Luo, L., Kreitzer, A.C., Nelson, A.B., 2018. A subpopulation of striatal neurons mediates levodopa-induced dyskinesia. Neuron 97, 787–795.e6.
Han, X., 2012. In vivo application of optogenetics for neural circuit analysis. ACS Chem. Neurosci. 3, 577–584.
Hernandez, L., Castela, I., Ruiz-DeDiego, I., Obeso, J.A., Moratalla, R., 2017. Striatal activation by optogenetics induces dyskinesias in the 6-hydroxydopamine rat model of Parkinson disease. Mov. Disord. 32, 530–537.
Hernandez, L.F., Kubota, Y., Hu, D., Howe, M.W., Lemaire, N., Graybiel, A.M., 2013. Selective effects of dopamine depletion and L-DOPA therapy on learning-related firing dynamics of striatal neurons. J. Neurosci. 33, 4782–4795.
Heumann, R., Moratalla, R., Herrero, M.T., Chakrabarty, K., Drucker-Colín, R., Garcia-Montes, J.R., Simola, N., Morelli, M., 2014. Dyskinesia in Parkinson's disease: mechanisms and current non-pharmacological interventions. J. Neurochem. 130, 472–489.
Kalia, L.V., Lang, A.E., 2015. Parkinson's disease. Lancet 386, 896–912.
Keifman, E., Ruiz-DeDiego, I., Pafundo, D.E., Paz, R.M., Solís, O., Murer, M.G., Moratalla, R., 2019. Optostimulation of striatonigral terminals in substantia nigra induces dyskinesia that increases after L-DOPA in a mouse model of Parkinson's disease. Br. J. Pharmacol. 176, 2146–2161.
Klaus, A., Martins, G.J., Paixao, V.B., Zhou, P., Paninski, L., Costa, R.M., 2017. The spatiotemporal Organization of the Striatum Encodes Action Space. Neuron 95, 1171–1180.e7.
Kravitz, A.V., Freeze, B.S., Parker, P.R.L., Kay, K., Thwin, M.T., Deisseroth, K., Kreitzer, A.C., 2010. Regulation of parkinsonian motor behaviours by optogenetic control of basal ganglia circuitry. Nature 466, 622–626.
Kubota, Y., Liu, J., Hu, D., DeCoteau, W., Eden, U., Smith, A., Graybiel, A., 2009. Stable encoding of task structure coexists with flexible coding of task events in sensorimotor striatum. J. Neurophysiol. 102, 2142–2160.
Lima, S., Hromádka, T., Znamenskiy, P., Zador, A., 2009. PINP: a new method of tagging neuronal populations for identification during in vivo electrophysiological recording. PLoS One 4.
Mallet, N., Schmidt, R., Leventhal, D., Chen, F., Amer, N., Boraud, T., Berke, J.D., Mallet, N., Schmidt, R., Leventhal, D., Chen, F., Amer, N., Boraud, T., 2016. Arkypallidal cells send a stop signal to striatum. Neuron 89, 308–316.
Mink, J.W., 1996. The basal ganglia: focused selection and inhibition of competing motor programs. Prog. Neurobiol. 50, 381–425.
Obeso, J.A., Rodriguez-Oroz, M.C., Rodriguez, M., DeLong, M.R., Olanow, C.W., 2000. Pathophysiology of levodopa-induced dyskinesias in Parkinson's disease: problems with the current model. Ann. Neurol. 47. S22-32; discussion S32-4.
Owen, S., Liu, M., Kreitzer, A., 2019. Thermal constraints on in vivo optogenetic manipulations. Nat. Neurosci. 22, 1061–1065.
Parker, J.G., Marshall, J.D., Ahanonu, B., Wu, Y.-W., Kim, T.H., Grewe, B.F., Zhang, Y., Li, J.Z., Ding, J.B., Ehlers, M.D., Schnitzer, M.J., 2018. Diametric neural ensemble dynamics in parkinsonian and dyskinetic states. Nature 557, 177–182.
Pavón, N., Martín, A.B., Mendialdua, A., Moratalla, R., 2006. ERK phosphorylation and FosB expression are associated with L-DOPA-induced dyskinesia in hemiparkinsonian mice. Biol. Psychiatry 59, 64–74.
Perez, X., Zhang, D., Bordita, T., Quik, M., 2017. Striatal D1 medium spiny neuron activation induces dyskinesias in parkinsonian mice. Mov. Disord. 32, 538–548.
Picconi, B., Hernández, L., Obeso, J., Calabresi, P., 2018. Motor complications in Parkinson's disease: striatal molecular and electrophysiological mechanisms of Dyskinesias. Mov. Disord. 33, 867–876.
Pons, R., Syrengelas, D., Youroukos, S., Orfanou, I., Dinopoulos, A., 2013. Levodopa-induced Dyskinesias in tyrosine hydroxylase deficiency. Mov. Disord. 28, 1058–1063.
Quinn, N., Parkes, D., Janota, I., Marsden, C.D., 1986. Preservation of the substanitia nigra and locus coeruleus in a patient receiving levodopa (2 kg) plus decarboxylase inhibitor over a four-year period. Mov. Disord. 1, 65–68.
Rothwell, P.E., Hayton, S.J., Sun, G.L., Fuccillo, M.V., Lim, B.K., Malenka, R.C., 2015. Input- and output-specific regulation of serial order performance by Corticostriatal circuits. Neuron 88, 345–356.

Ryan, M.B., Bair-Marshall, C., Nelson, A.B., 2018. Aberrant striatal activity in parkinsonism and levodopa-induced dyskinesia. Cell Rep. 19, 3438–3446.e5.
Suárez, L.M., Alberquilla, S., García-Montes, J.R., Moratalla, R., 2018. Differential synaptic remodeling by dopamine in direct and indirect striatal projection neurons in Pitx3−/− mice, a genetic model of Parkinson's disease. J. Neurosci. 38, 3619–3630.
Taverna, S., Ilijic, E., Surmeier, D.J., 2008. Recurrent collateral connections of striatal medium spiny neurons are disrupted in models of Parkinson's disease. J. Neurosci. 28, 5504–5512.
Togasaki, D.M., Tan, L., Protell, P., Di Monte, D.A., Quik, M., Langston, J.W., 2001. Levodopa induces dyskinesias in normal squirrel monkeys. Ann. Neurol. 50, 254–257.
Togasaki, D.M., Protell, P., Tan, L.C.S., Langston, J.W., Di Monte, D.A., Quik, M., 2005. Dyskinesias in normal squirrel monkeys induced by nomifensine and levodopa. Neuropharmacology 48, 398–405.